Journal of Marine Research, 53, 647–674, 1995

Mesoscale distribution of zooplankton in the California Current in late spring, observed by Optical Plankton Counter

by Mark E. Huntley[1], Meng Zhou[1] and Walter Nordhausen[1]

ABSTRACT

A survey of zooplankton in the upper 300 m of the central California Current, from the coastal shelf to 128W and between 36.5N and 39.5N, was conducted in early June 1993 using an Optical Plankton Counter (OPC) as part of an interdisciplinary study of mesoscale ocean circulation and biological dynamics. The OPC was part of a multi-instrument package towed on an undulating vehicle (SeaSoar). Estimates of normalized size spectra and absolute abundance from OPC data compared favorably with measurements based on Bongo net catches. After processing, the standardized OPC data set provides a resolution of ≈ 7 km in the horizontal and 10 m in the vertical for 60 size categories of zooplankton ranging in estimated body weight from 3 μg C to 3000 μg C. Results reveal rich mesoscale variability in zooplankton distributions at scales of 30–60 km, with regions of enhanced biomass and abundance coinciding with the location of mesoscale eddies, both cyclonic and anticyclonic. The central jet of the California Current departed from the coastline near Cape Mendocino (39.5N), separating a region of generally greater zooplankton biomass near the coast from one of lower biomass to the west. The jet usually contained lower biomass than adjacent eddies. Total zooplankton biomass ranged from <2 g C m^{-2} to >20 g C m^{-2}. The two mesoscale features containing the highest biomass, one 200 nm offshore of Cape Mendocino and another 100 nm west of Monterey Bay, were dominated by euphausiids.

1. Introduction

Zooplankton in the size range from 500 μm to 30 mm body length (small copepods to euphausiids) constitute the principal trophic link between primary production and fish production in the California Current. The mesoscale distribution of zooplankton in this eastern boundary current, and the physical dynamics that cause it, are therefore critical in determining where and when food will be available to fishes. Such was the primary motivation for including studies of zooplankton distributions in the decades-long CalCOFI (California Cooperative Fisheries Investigations) program.

1. Marine Biology Research Division, Scripps Institution of Oceanography, 0202, La Jolla, California 92093, USA.

The initial perception of the California Current as a broad and relatively sluggish, uniform circulation feature (Sverdrup *et al.,* 1946) was not greatly changed by results of the first quasi-synoptic surveys (Hickey, 1979; Wyllie, 1966). However, with the advent of satellite oceanography in the late 1970s it became immediately evident that the entire current system, especially in the region from Cape Blanco to Point Conception, was rich in mesoscale jets and eddies (Bernstein *et al.,* 1977) that have a significant effect on the distribution of phytoplankton (Peláez and McGowan, 1986). The potential of advective processes in such mesoscale features to alter the distribution of zooplankton could be inferred from models (Mooers and Robinson, 1984) or from Lagrangian drifter observations (Poulain and Niiler, 1989), but direct evidence has only recently become available.

There has never been a quasi-synoptic description of the distribution of zooplankton over a broad region of the California Current that is resolved at the mesoscale. The wide-ranging CalCOFI surveys have provided excellent descriptions of the regional distributions of copepods (Fleminger, 1964) and euphausiids (Brinton, 1962) by species. Furthermore, the distribution of total zooplankton displacement volume caught in 505-μm mesh nets has been described for a single year of eight successive CalCOFI surveys (Smith, 1974). However, these studies fail to resolve mesoscale features because the standard station spacing employed in most of the CalCOFI survey area (≈ 65 km) is simply too great.

The transport and redistribution of zooplankton by mesoscale circulation processes in the California Current are clear from a number of recent studies focused on isolated features. An eddy offshore of Point Conception was found to contain colder water zooplankton typical of coastal waters, from which cross-shelf transport was inferred (Haury, 1984). A narrow coastal jet off Point Arena, <30 nm across, was found to contain zooplankton species in its cold water core that did not occur on either side (Mackas *et al.,* 1991), and had a demonstrated effect on the productivity of the copepod *Eucalanus californicus* (Smith and Lane, 1991). The jet, which moved more rapidly (>1.0 m s^{-1}) by one order of magnitude than the mean flow of a classical eastern boundary current, appeared from satellite imagery and drifter tracks to flow several hundred km offshore, while connecting to a number of eddies as it meandered more than 700 km southward (Huyer *et al.,* 1991; Kosro *et al.,* 1991).

How does the mesoscale variability in circulation of the California Current affect the distribution and dynamics of zooplankton? The recent studies of isolated mesoscale features (e.g. Haury, 1984; Mackas *et al.,* 1991) provide good examples of representative processes, but from which larger scale zooplankton distributions can only be inferred. Conversely, the study area of the CalCOFI program, while adequately large, has been too coarsely sampled to allow distributions to be resolved at smaller scales where mesoscale physical forcing occurs. What is required is a study over an area sufficiently large to encompass the principal domain of southward

transport in the California Current, and at the same time sampled at a resolution that allows a number of representative mesoscale features to be adequately defined.

Here we report on the results of a field study conducted in June 1993 over a 100,000 km^2 region of the Pacific Ocean off coastal northern California between 36.5 and 39.5N and extending westward approximately 200 nm to 128W. The study of zooplankton was one part of the interdisciplinary Eastern Boundary Current (EBC) program, which included simultaneous studies of both biological and physical oceanography. To obtain samples of zooplankton at sufficiently high spatial resolution using traditional net capture techniques would have been prohibitive in terms of time and cost of subsequent sample analysis. Therefore, we employed an Optical Plankton Counter (OPC; Focal Instruments, Dartmouth, Nova Scotia). This instrument has the capability of sizing zooplankton in the range of 250 μm to 14 mm equivalent spherical diameter, equal to approximately 500 μm to 28 mm in length, and measuring particle abundance in that range at 0.5-sec intervals as it is towed through the water at a speed of 5–8 kts (Herman, 1992). Aside from the high data rate, one of the advantages of this instrument for our study was that it could be mounted on the same towed body (SeaSoar; Chelsea Instruments, East Molesey, Surrey, UK) that carried all other underwater instruments (e.g. CTD), and therefore physical and biological measurements could be used to characterize the same environment, sampled at the same temporal and spatial scales.

One potential disadvantage of the OPC is that, being based on measurements of light transmission, the data it produces cannot distinguish between biotic and abiotic particles (Herman, 1988). Thus, any detrital material and inorganic particles that are counted might falsely be considered as zooplankton, and therefore could corrupt one's interpretation of the data. In numerous deployments in the North Atlantic, however, the OPC has been clearly demonstrated to faithfully reproduce the distributions and abundances of zooplankton estimated from samples collected with a multiple net system, BIONESS (Herman, 1992). Furthermore, even the abundance of individual developmental stages of the copepod *Calanus finmarchicus* estimated by the OPC compared favorably with those measured by microscope counts of samples collected with a net towed at the same location (Herman, 1992). However, these encouraging results do not dispel the concern that in the California Current system the OPC might not provide an equally faithful enumeration of zooplankton.

In this paper we critically examine the ability of the OPC to faithfully reproduce zooplankton size frequency distributions based on samples taken from the same region with nets. We then describe the procedures that were used to integrate measurements at temporal and spatial scales appropriate to both the limits of the instrument and its scientific purpose. Finally, we report on the distributions of zooplankton in the California Current during late spring and early summer, and discuss these results in relation to features of the mesoscale circulation.

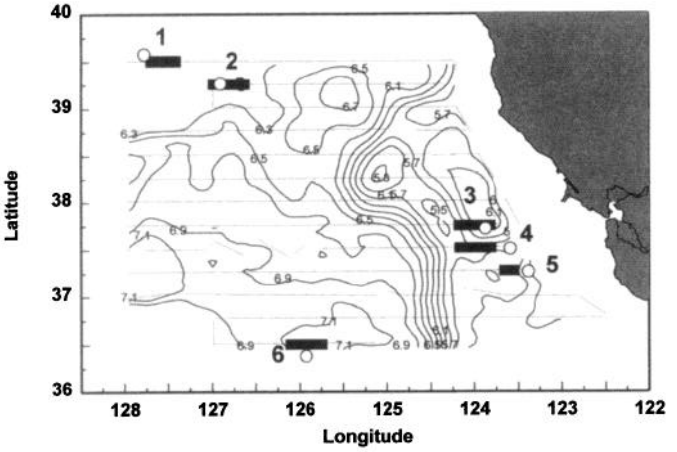

Figure 1. Study area, central California Current region, June 1993. Longitudinal transect lines at intervals of 0.25° of latitude represent the cruise track of the R/V *Wecoma* as it towed the instrumented SeaSoar from north to south. Dynamic topography at 11 db relative to 295 db shows the central jet of the California Current meandering between 124 and 125W (from Kosro *et al.,* 1994). Open circles represent stations at which Bongo tows were made, and thickened lines on the transect show the corresponding distance along which OPC data were averaged for comparison to Bongo data.

2. Methods

a. Deployment of the Optical Plankton Counter. Our use of the OPC marked the first time that it has ever been mounted on SeaSoar. The instrument was mounted beneath the SeaSoar body in a fashion similar to that described for mounting on Batfish (Herman, 1988; Fig. 4), with the exception that the beveled edge of the OPC sampling aperture was made to face downward rather than upward. On the SeaSoar, this configuration reduced drag and yielded a more stable flight pattern.

The large-scale survey of the California Current was carried out in a series of onshore-offshore transects beginning June 1, 1993 at 39.5N and ending June 28 at 36.15N (Fig. 1). The survey was interrupted by 40 h of severe weather (June 17–19) and by a 52-h port call in San Francisco (June 19–21) before completing the four southernmost transects. The instrument package aboard SeaSoar included OPC, CTD, PAR and *in vivo* fluorometer; after the stop at San Francisco the fluorometer was replaced with a TOFU (TOwed Fluorescence Unit). In this paper we report only on our own measurements with the OPC.

In normal operating conditions the SeaSoar was towed at a velocity of 8 kts while it undulated from near the surface (<5 m depth) to almost 300 m. The time to complete a full undulation cycle, surface to surface, was ≈ 8 min, during which period the distance transited was on average 1.96 km. Thus, in less than 6 h the instruments transited one degree of longitude (≈ 45 nm at these latitudes), performing a total of more than 70 continuous profiles of the upper 300-m water column.

SeaSoar was generally operated continuously for several days at a time. However, whenever the vehicle was brought aboard we used a Bongo net (155 μm mesh) fitted with a calibrated flowmeter to collect zooplankton in an oblique haul from 300 m to the surface. Samples were preserved in borate-buffered 5% formalin for later analysis. Bongo tows were made in six areas throughout the survey region (Fig. 1).

b. Data integration. Interpretation of OPC data is greatly facilitated by integration over appropriate scales, resulting in a format that is standardized with respect to vertical and horizontal distances. This is especially important when, as in our case, one desires to incorporate in the database other data sets which are also in standard format (e.g. CTD data).

The overriding concern in data integration is to achieve the highest possible spatial resolution, while conserving a high degree of resolution in particle size spectra with respect to particle size. The OPC raw data stream partitions particles into 4096 size categories. Although size and abundance data are continuously transmitted, a time stamp is inserted only every 0.5 sec, which sets the lowest time limit for fixing the spatial location of a given measurement of particle abundance. The total counts in any 0.5-sec interval were generally in the range from 10 to 100. Therefore, both the size categories and the time period were integrated over larger intervals to provide statistically meaningful size spectra (discussed below). We integrated the size spectral data into 60 size classes of equal increments with respect to equivalent spherical diameter, such that each size category increased by 230 μm in diameter over the range from 270 μm to 13.8 mm. Given a width:length ratio for zooplankton (W. Nordhausen, unpubl. data), and using Herman's (1992) equation for the relation between length, width and equivalent spherical diameter, this equates to size classes of zooplankton which increase by ≈ 500 μm in length over the size range from 540 μm to 28 mm. In the California Current region this size range extends from small copepods (e.g. *Acartia* copepodids) to euphausiids (e.g. *Euphausia pacifica*).

The OPC included a pressure sensor to provide depth data at 0.5-s intervals, and was also linked to the shipboard Global Positioning System (GPS) unit, as were other sensors aboard the SeaSoar. Both pressure and GPS data were incorporated into the OPC raw data stream. Unfortunately, we lost OPC depth readings on the first day of the cruise due to the failure of two diodes, and therefore obtained depth data from the CTD database by matching GPS locations of the two data sets.

We determined the maximum vertical resolution of OPC data from its maximum diving speed. Although the average vertical velocity of the SeaSoar was only 1.3 m s^{-1}, it tends to remain at more or less constant depth at the top and bottom of its undulation cycle, and dives at velocities approaching 5 m s^{-1}. Given the OPC time stamps at 0.5-sec intervals, we felt it was necessary to insure a minimum of several size spectra per depth interval, and thus selected a vertical resolution of 10 m.

The maximum possible horizontal resolution is constrained by two important

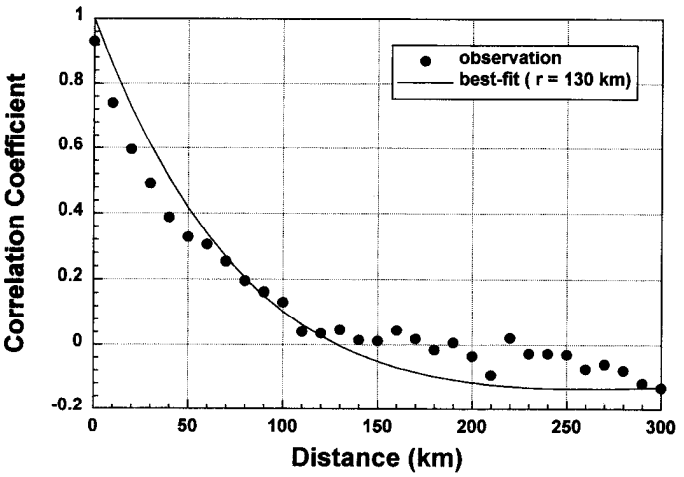

Figure 2. Results of autocorrelation analysis of standardized OPC data, with model of Eq. 3 (—) fitted to data (●).

criteria: first by statistical requirements for a sufficiently large sample volume, and second by the decorrelation scale of features. Furthermore, although the along-transect horizontal resolution is potentially quite high, it is limited for the purpose of interpolation by the north-south distance between successive transects (15 nm). The necessary sample volume is dictated by the abundance of animals, which, over more than 50% of the size range measured by the OPC, was $<1\ m^{-3}$. The greater the volume sampled, the more accurate is the resulting size spectrum. For Bongo tows, the volume sampled was approximately $300\ m^3$. In order to obtain statistically comparable size spectra, a similar volume must be sampled by the OPC. The cross-sectional area of the OPC sample tunnel is $0.0066\ m^3$, so the OPC would need to travel ≈ 45 km to sample a volume equivalent to that sampled by a standard Bongo tow. Horizontal integration of OPC data was therefore necessary, but, recognizing that such integration might eliminate some small scale features, we used a rigorous approach to obtain the highest resolution possible.

Autocorrelation analysis provides one method by which to determine the upper limit of the horizontal integration range. To conduct this analysis (described below in detail), we first chose to integrate OPC data over 10 km in along-transect distance—equal to approximately 16 km of travel by the undulating OPC—and thus provided a sample volume of $\approx 100\ m^3$. The autocorrelation coefficient based on this integrated data series is 0.74 at 10 km (Fig. 2). The result implies that integration over horizontal distances >10 km may incorporate features which are not correlated. As a compromise between the sufficiently large sample size required for statistically meaningful size spectra, and a sufficiently short horizontal integration that would distinguish uncorrelated features, we chose a horizontal integration distance of 0.1° in longitude, or approximately 7 km.

The details of autocorrelation analysis with respect to different scales of features are well known (Bretherton *et al.*, 1976; Clancy, 1983; Mooers and Robinson, 1984; Robinson *et al.*, 1984). The autocorrelation shown in Figure 2 might be best-fit by the function

$$\left(1 - \frac{|x|^2}{R^2}\right) \exp\left(-\frac{x^2}{2R^2}\right) \tag{1}$$

where x is the distance and R is the decorrelation scale (Mooers and Robinson, 1984; Robinson *et al.*, 1984; Carter and Robinson, 1987). The best fit to the data yields $R =$ 78 km. However, Eq (1) does not provide a good fit to our data; it overestimates the correlation when the distance is <60 km, and underestimates it when the distance is >60 km.

In our survey region of the California Current there are different characteristic scales for different features, such as the scales of eddies with different origins, scales along and across the jet, and the scale of the general tendency for zooplankton abundance to decrease in the offshore direction. An analytical function that allows analysis of these several scales might be

$$\sum_{i=1} A_i \left(1 - \frac{|x|^2}{R_i^2}\right) \exp\left(-\frac{|x|^2}{2R_i^2}\right) \tag{2}$$

where A_i is the weight for scale R_i. However, the detailed analysis of scales is not the purpose of this article. Here we are only interested in obtaining a first order approximation of the autocorrelation function, which provides the basis for the spatial interpolation we performed.

Following the discussion by Bretherton *et al.* (1976) and Clancy (1983), the autocorrelation function must be positive definite (i.e. >0). Therefore, instead of using either Eqs. (1) or (2), we used the following analytical formula:

$$\left(1 - \frac{|x|}{R}\right) \exp\left(-\frac{|x|}{R}\right) \tag{3}$$

Figure 2 shows the best fit of Eq. (3), with $R = 130$ km. Obviously, Eq. (3) provides a better fit to the data than Eq. (1). The averaging in space of these data is unavoidable because of the small intake area of the OPC sampling tunnel. Such integration will eliminate any features on scales of less than 0.1° of longitude, and will not eliminate any features on scales larger than this. Furthermore, this analysis implies that, in our survey area, the averaged spatial scale of the dominant features is 130 km.

Thus, in our standardized OPC data set, each data point represents size spectral data reduced from 4096 to 60 size categories, averaged over 10 m intervals in the vertical and over 0.1° of longitude, or ≈ 7 km, in the horizontal.

c. Analysis of zooplankton samples and comparison to OPC data. Preserved samples were analyzed by passing each entire sample through a series of successively smaller Nitex mesh screens of the following pore sizes: 3300, 1000, 800, 500, 300 and 200 μm. The subsample retained on each screen was then enumerated, yielding a size spectrum with the foregoing size categories. Euphausiids dominated the zooplankton >3 mm in length, and these were identified to species, enumerated and individually sized in each sample to yield a frequency distribution of large zooplankton in length increments of 0.5 mm.

Abundances of zooplankton captured in Bongo tows were calculated from the total counts in each size category divided by the total volume of water filtered, measured by a calibrated flowmeter. Abundances of particles sampled by the OPC were calculated based on the assumption that the volume 'filtered' is the product of the cross-sectional area of the sampling aperture and the distance traveled by the OPC, as recommended by Herman (1992). This procedure normalized the units to allow comparison between Bongo and OPC samples.

To facilitate comparisons between net catch estimates and OPC estimates of zooplankton size spectra and biomass we took the average of several successive 0.1°-longitude OPC size spectra in the area nearest to where Bongo tows were made, taking into account the prevailing physical circulation patterns. Thus, if a Bongo tow was made in an eddy adjacent to the central jet of the California Current (Fig. 1), we took care to include OPC data only along the relevant line of latitude within the eddy. This procedure amounted to averaging over no more than three to five successive OPC size spectra in the standardized data set, but it allowed the total volumes filtered by both instruments to be of the same order.

In order to allow comparison to both theoretical and observed particle size spectra in aquatic systems (Platt and Denman, 1978; Sprules *et al.,* 1991), it is most useful to express body size in terms of weight. We selected units of body carbon which, in addition, permits useful comparison in terms of trophodynamics. To make the conversion we applied the equation of Rodríguez and Mullin (1986), i.e.

$$\log \text{wt } (\mu\text{g C}) = 2.23 \log \text{length } (\mu\text{m}) - 5.58 \quad (4)$$

Conversions were made from net sample data using microscopic measurements of body length, and from OPC data using length inferred from estimates of equivalent spherical diameter as previously stated.

3. Results

a. Comparison of zooplankton size-frequency distributions: OPC vs. net catch data. Normalized size spectra (*sensu* Platt and Denman, 1978) from both OPC and Bongo data yielded essentially the same result in the six areas where comparisons were made (Fig. 3), with the exception of Area 1, where the coefficient of determination was low and the slope of the relationship was substantially less than those for the

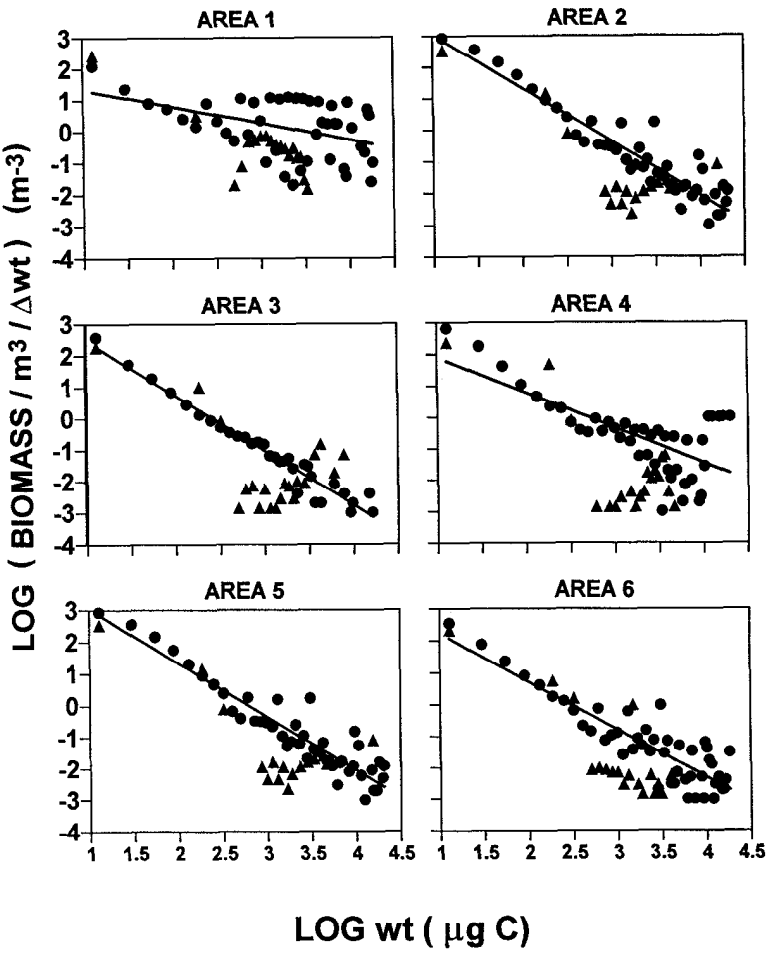

Figure 3. Normalized size spectra of OPC (●) and Bongo data (▲) over the range of observed body sizes in Areas 1–6, shown in Figure 1. Regression equations for OPC data are presented in Table 1.

remaining five areas (Table 1). In all cases there was generally very good agreement between the counts of small particles sampled by the OPC and small zooplankton sampled by nets. However, with the increase in variance for larger size classes of zooplankton (> 1 mg C body weight), estimates of abundance from the Bongo net catches tended to be lower than those from the OPC. It is possible this may have been due to avoidance by larger zooplankton of the Bongo net, which traveled at only 2 kts, by comparison to the high speed of the OPC (8 kts).

A comparison of OPC and Bongo estimates of the abundance in each size category yielded correlation coefficients up to 0.84 (Fig. 4; Table 2). Correspondence between the two data sets appeared especially good at abundances $> 0.1\ m^{-3}$. The poor

Table 1. Regression equations for OPC normalized size-spectra in Areas 1–6, where Bongo net tows were also made (see Fig. 1). Abundance (numbers m^{-3}) was plotted against body weight (μg C), and fitted with the model: $\log N = \log x + y \log W$, where N is abundance and W is body weight. Regression equations correspond to relationships shown in Figure 3.

Area	y	$\log x$	r^2
1	1.867	−0.533	0.20
2	4.797	−1.961	0.96
3	4.238	−1.752	0.96
4	3.035	−1.123	0.50
5	4.743	−1.700	0.89
6	3.750	−1.514	0.80

relationship at low abundances is almost certainly due to undersampling by both instruments; given the volume filtered by either instrument, an abundance estimate of 0.05 m^{-3} represents a total sample of only 10–20 animals, and therefore a change of only ±1–2 animals in the total sample would alter the estimate by 10%.

b. Day-night comparisons. One of the questions that could be raised regarding any continuous sampling of the spatial distribution of marine zooplankton is whether the results are biased by diel vertical migration. Specifically, we are interested in

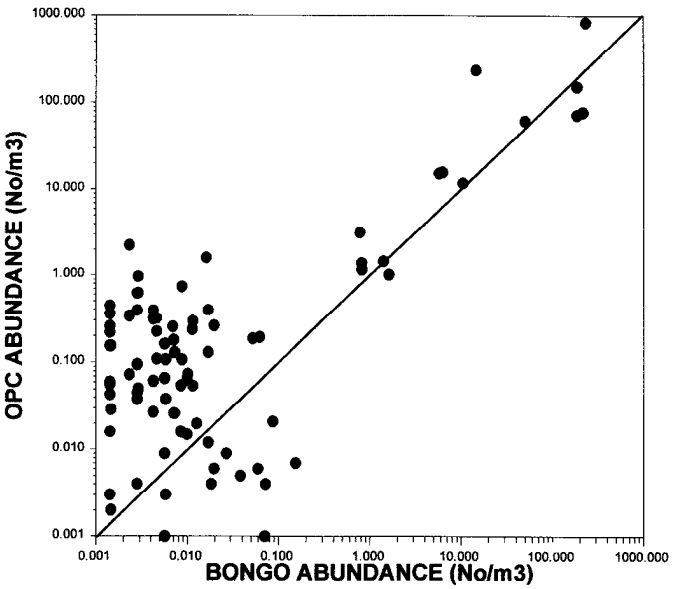

Figure 4. Estimates of zooplankton abundance (numbers m^{-3}) from OPC measurements as a function of the same estimate from Bongo net samples. Different symbols represent the six different areas for which regression equations are given in Table 2. Regression for pooled data also given in Table 2. The solid line represents a 1:1 relationship.

Table 2. Regression equations for estimates of zooplankton abundance from OPC measurements as a function of Bongo net tow measurements in Areas 1–6. Equations were fit to the model: $\log N_{OPC} = \log x + y \log N_{BGO}$, where N_{OPC} is the abundance from OPC measurements and N_{BGO} is the abundance from corresponding Bongo tows. Regression equations correspond to the data shown in Figure 4.

Area	y	$\log x$	r^2
1	0.530	−1.175	0.22
2	0.795	−0.247	0.72
3	0.706	−0.842	0.38
4	1.131	−1.225	0.71
5	1.136	−1.505	0.84
6	0.974	−1.007	0.62

estimating the total biomass in the upper 300 m of the water column, so we are concerned that upward migration of animals from below this layer might cause regular increases in night-time estimates of total zooplankton biomass. If this were true, then it would create a systematic bias in our estimate of the spatial distribution patterns of zooplankton.

We tested for a potential bias due to diel vertical migration in the following way. First we divided all standardized, 0.1°-longitude OPC samples into day and night, using integrated water column (0–300 m) values for both abundance (numbers m^{-2}) and biomass (g C m^{-2}). "Day" samples were deemed to be those falling between 05.00 h and 19.00 h local time, which approximately represent the times at dawn and 1 hour prior to sunset. These times were chosen because many zooplankton species are known to begin their upward vertical migration with the rapid decrease in daylight and to resume their daytime position in the water column just before sunrise (Banse, 1964). "Night" samples occupied the remaining portion of the 24-h day. This yielded a total number of 498 OPC samples, with 281 in the day and 227 at night. Second, we divided the total range (0–600,000 numbers m^{-2}) of abundance estimates into 15 equal categories, and did the same for the entire range of biomass observations (0–15 g C m^{-2}). The resulting frequency distributions for both abundance (Fig. 5A) and biomass (Fig. 5B) demonstrate no systematic differences. If significant biomass of zooplankton were migrating into the upper 300 m of the water column at night we would expect the frequency distribution of night-time samples to be skewed toward values of greater biomass. However, such is not the case, and we therefore conclude that diel vertical migration, if it occurred, did not significantly bias our interpretation of the spatial distribution of either zooplankton abundance or biomass in the upper 300 m.

c. Objective interpolation for horizontal mapping. For mapping of vertical cross-sections we used the processed OPC data, i.e. with 10 m vertical resolution and 0.1°-longitude horizontal resolution, and contoured these directly using Stanford

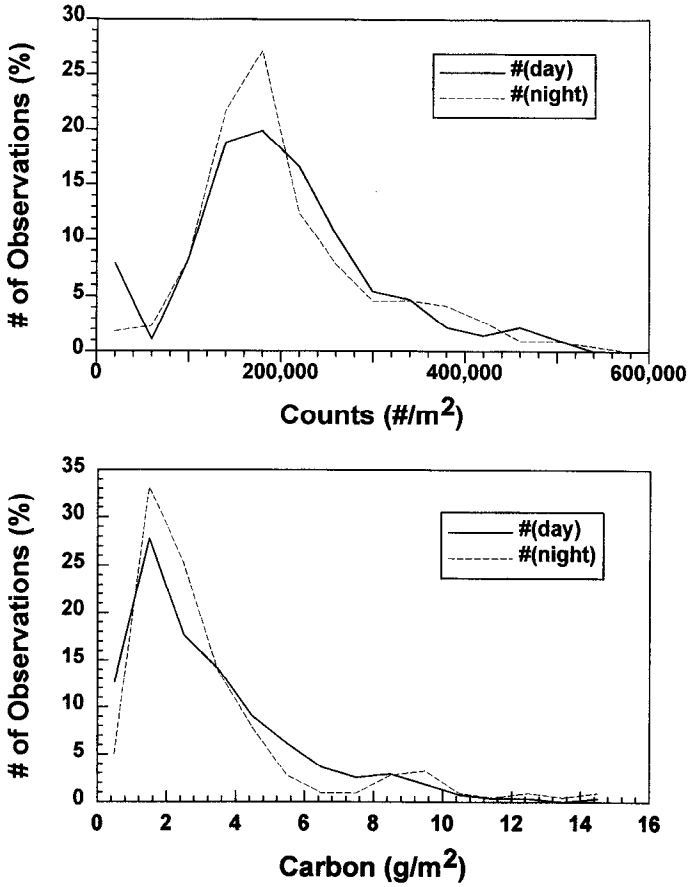

Figure 5. Frequency distributions of (A) abundance and (B) biomass estimates (numbers m^{-2} and g C m^{-2}, respectively) from standardized OPC data, averaged over 0.1° of longitude for 281 night samples and 227 day samples. The similarity in frequency distributions suggests that there was no detectable vertical migration of zooplankton into the upper 300 m layer at night.

Graphics®. However, for horizontal mapping, interpolation was necessary to obtain smooth contours, due to low resolution in the north-south direction. The final matrix before contouring by Stanford Graphics® was 50 × 40 in longitude and latitude, respectively, in the domain from 123–128W and 36.5–39.5N, corresponding to approximately 7 × 7 km. The objective interpolation method we used is based on that of Bretherton *et al.* (1976) and the autocorrelation function given by Eq. (3).

For interpolation, we have assumed that a measurement ϕ_r is the true value, θ_r, plus some random noise, e_r:

$$\phi_r = \theta_r + e_r \tag{5}$$

where subscript r represents the location at r and the error term, e_r, is uncorrelated with the error of the measurements at location s and with the field θ, i.e.

$$\overline{e_r\varphi_s} = 0$$
$$\overline{e_re_s} = \epsilon^2\delta_{rs} \qquad (r, s = 1, 2, \ldots, n) \tag{6}$$

where ϵ^2 is the error variance, δ_{rs} is defined as equal to zero when $r \neq s$ and equal to 1 when $r = s$, and n is the number of observations. The least-squares optimal estimation for θ is:

$$\hat{\theta} = \sum_{r=1}^{n} C_{xr}\left(\sum_{\delta=1}^{n} A_{rs}^{-1}\varphi_s\right) \tag{7}$$

where $\hat{\theta}$ is an estimate of θ at x, where

$$A_{rs} = \overline{\varphi_r\varphi_s} = F(x_r - x_s) + \epsilon^2\delta_{rs} \tag{8}$$

is the matrix of correlation between all pairs of observations, and where

$$C_{xr} = \overline{\theta_x\varphi_r} = F(x_x - x_r) \tag{9}$$

is the correlation between the quantity θ_x to be estimated and the rth measurement.

As mentioned earlier, the primary intent of this paper is not to discuss objective mapping and error analysis, so Eqs. (5) through (9) are provided only for clarifying the approach we used. Eq. (3) was used as the analytical correlation function, which represents the scale of major features in our survey area. We also simply assumed $\epsilon^2 = 0$ to force the estimate $\hat{\theta}_r$ equal to ϕ_r at the rth observation.

d. Horizontal distributions of zooplankton in relation to dynamic topography. Most features of the horizontal distribution of zooplankton abundance were clearly related to identifiable circulation features evident in the dynamic topography. First we define each of these features with respect to the horizontal distribution of zooplankton abundance (Fig. 6) and biomass (Fig. 7) integrated over the total 300 m water column. The size composition with respect to body carbon weight of each one of these features is then also considered (Fig. 8). Finally, we show vertical cross-sections, with 10-m vertical resolution, of several representative features (Figs. 9–13).

The horizontal distribution of vertically integrated zooplankton abundance (Fig. 6) corresponds to four key features evident in the physical oceanographic data. In general, the central jet of the California Current separated a region of low abundance offshore from a region of enhanced coastal abundance. Within each of these general regions, however, certain isolated features are apparent. The abundance maximum centered at 39.2N, 125.5W coincides with the *northern anticyclonic eddy* observed at the same location. The *cyclonic eddy* on the coastal side of the jet at 38.4N also contained enhanced abundance of zooplankton. Offshore of Monterey

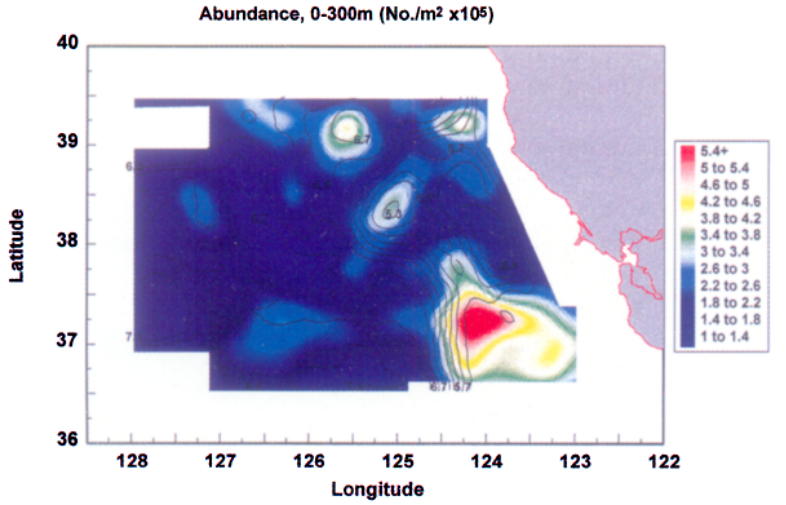

Figure 6. Vertically-integrated OPC measurements of total zooplankton abundance (numbers $\times 10^5$ m^{-2}) in the upper 300 m. Contours of dynamic topography are overlaid on false color contours of zooplankton abundance. Horizontal resolution of the standardized OPC data set was 7.2 km along the survey transects (Fig. 1).

Bay, again on the coastal side of the jet, was the greatest enhancement of zooplankton abundance within the entire survey area ($\approx$600,000 numbers m^{-2}); this coincided with the location of a large *coastal anticyclonic eddy* that Acoustic Doppler Current Profiler (ADCP; RD Instruments, San Diego) measurements showed to be

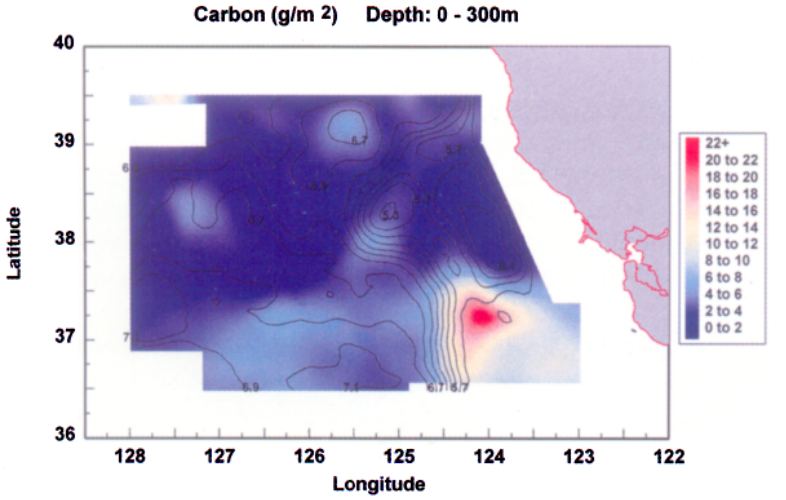

Figure 7. Vertically-integrated OPC measurements of total zooplankton biomass (g C m^{-2}) in the upper 300 m. Contours of dynamic topography are overlaid on false color contours of zooplankton biomass.

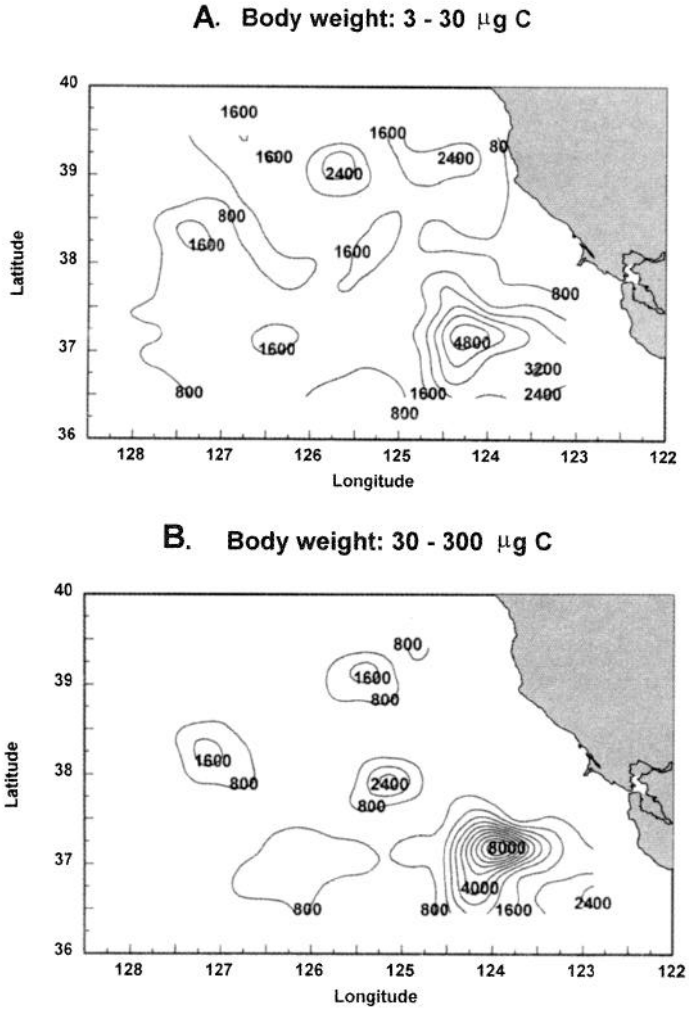

Figure 8. Vertically-integrated OPC measurements in the upper 300 m of zooplankton biomass (g C m^{-2}) by size category, for body weights in the range of (A) 3–30 μg C; (B) 30–300 μg C; and (C) 300–3000 μg C.

centered at approximately 37.2N, 124W (Kosro *et al.,* 1994). We also observed a peak in abundance, the *northern coastal maximum* at 39.2N, 124.4W, that coincided with the area where the jet appeared to depart from the coast.

The horizontal distribution of vertically integrated zooplankton biomass (Fig. 7) highlights some of the same features already observed in the distribution of zooplankton abundance, but brings new ones to light as well. The biomass of the *northern anticyclonic eddy* was >4 g C m^{-2}, that of the *cyclonic eddy* was also >4 g C m^{-2}, while that of the *coastal anticyclonic eddy* was >20 g C m^{-2}. In addition, a *northern*

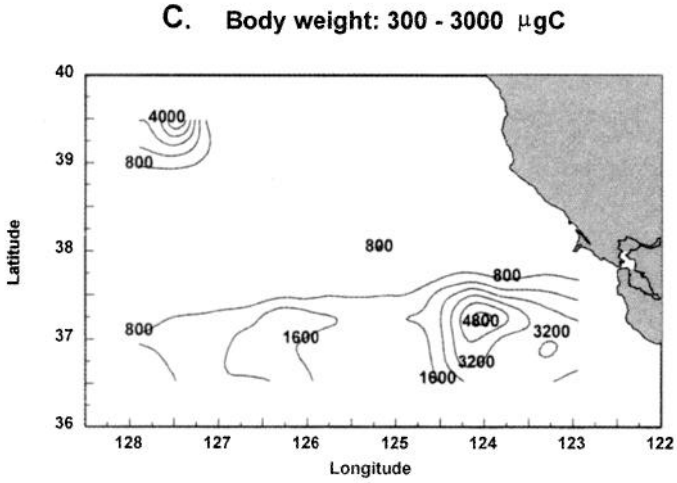

Figure 8. (Continued)

offshore maximum, centered at 39.5N, 127.5W had biomass exceeding 10 g C m^{-2}, but did not coincide with any dynamic feature that was obvious from physical oceanographic observations. The locations of both the *central offshore maximum* at 38.3N, 127.4W, with biomass >4 g C m^{-2}, and the *southern offshore maximum* at 37.1N, 126.4W, with biomass up to 6 g C m^{-2}, coincided with features of the dynamic topography that were only weakly evident. In general, the central jet of the California Current appeared to have relatively low integrated biomass of approximately 2 g C m^{-2}.

4. Composition of key biological/physical features in the northern California Current

Here we discuss the composition of each of the apparent biological features in the survey area with respect to depth distribution and size distribution in three categories of body carbon weight (3–30 μg; 30–300 μg; and 300–3000 μg). Most of our net samples were dominated by copepods and euphausiids, with chaetognaths, amphipods and gelatinous zooplankton making up only a small fraction of the total taxonomic composition. For convenience, we refer to the smallest size category as "small copepods," the medium category as "large copepods," and the largest category as "euphausiids." Although this nomenclature may oversimplify the taxonomic composition, it is generally supportable. For example, within the genera known to occur off California, the smallest size category would contain adults of *Paracalanus* spp. and *Acartia* spp. ($\approx$3 μg C; Checkley, 1980; Miller *et al.,* 1977), late copepodites and adults of *Pseudocalanus* spp. (up to 10 μg C; Frost, 1980; Ohman, 1985), all late copepodid stages of *Labidocera trispinosa* (up to $\approx$30 μg C; Barnett,

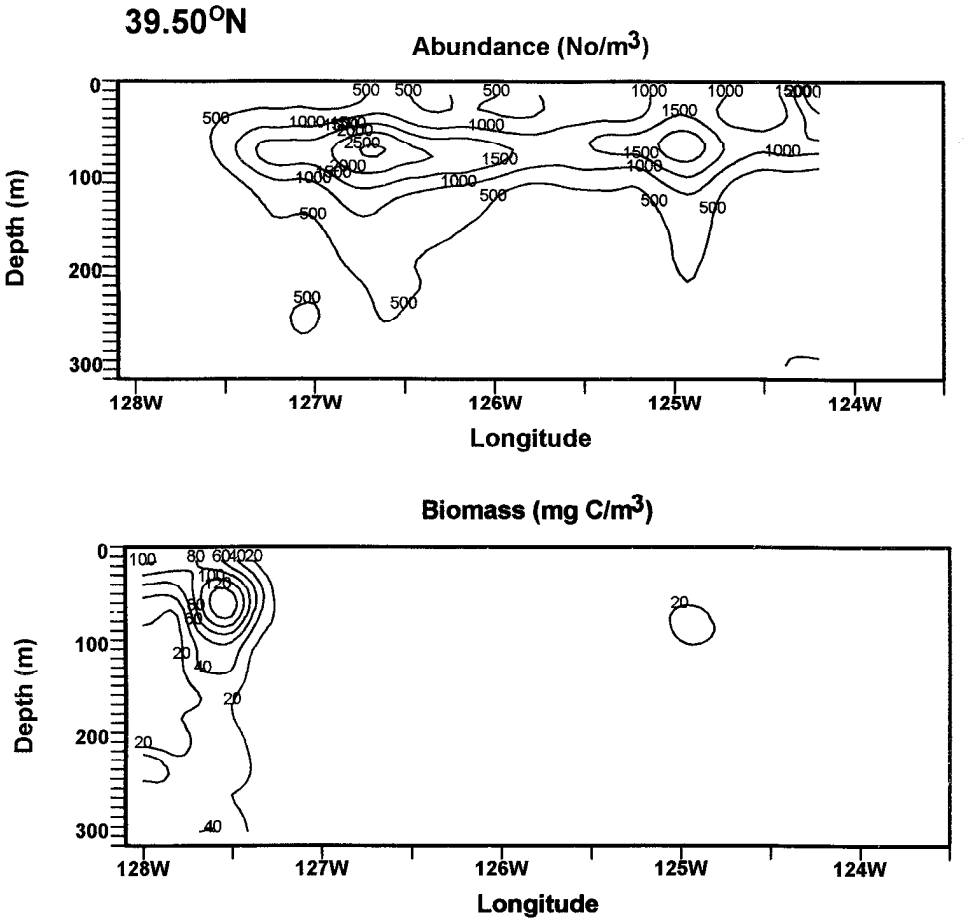

Figure 9. Vertical distribution of zooplankton abundance (numbers m^{-3}) and biomass (mg C m^{-3}) along 39.5N, resolved at 7.2 km in the horizontal and 10 m in the vertical.

1974) and most of the copepodid stages of *Calanus pacificus* (3.3 μg C at CII through 31.6 μg C at CV; Mullin and Brooks, 1970). The second size category, 30–300 μg C, could contain adults of *C. pacificus,* late developmental stages and adults of *Rhincalanus nasutus* (up to ≈150 μg C; Landry, 1983), and species such as *Neocalanus plumchrus* (≈200 μg C; Fulton, 1973) or the slightly larger *N. cristatus* (Vidal and Smith, 1986). The largest size category, 300–3000 μg C, would contain adult copepods of only a few of the largest species in the area, but would be dominated by euphausiids.

Each notable feature of the biological distribution is also considered here with respect to related features of the physical circulation, using dynamic topography as the primary reference point.

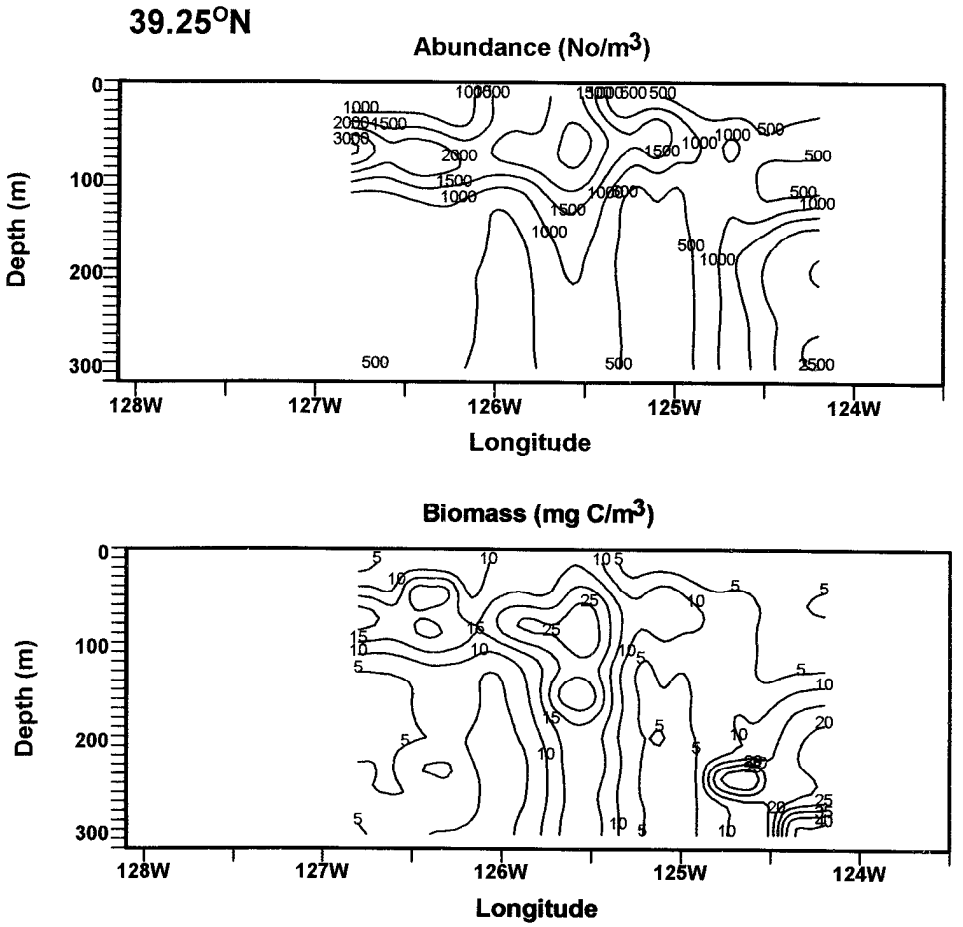

Figure 10. As in Figure 9, along 39.25N.

a. Northern offshore maximum (39.5N, 127.5W). With respect to carbon biomass, this feature contained the second largest concentration of zooplankton in the survey region (Fig. 7), although abundance was not very great (Fig. 6). Biomass was concentrated in the upper 100 m, with a maximum at 50 m exceeding 120 mg C m^{-3} (Fig. 9). The biomass was dominated by zooplankton in the largest size range, 300–3000 μg C (Fig. 8C), suggesting that these were probably euphausiids rather than copepods. Indeed, Bongo net tows in this area yielded abundances of euphausiids that were matched only by those found in the large anticyclonic eddy west of Monterey Bay. Eight species were present, with five of these, in order of relative abundance—*Thysanoessa gregaria, Nematobrachion flexipes, Euphausia pacifica, E. mutica* and *E. recurva*—accounting for >80% of the total abundance. No distinct physical oceanographic feature was obvious at this location, but that may have been

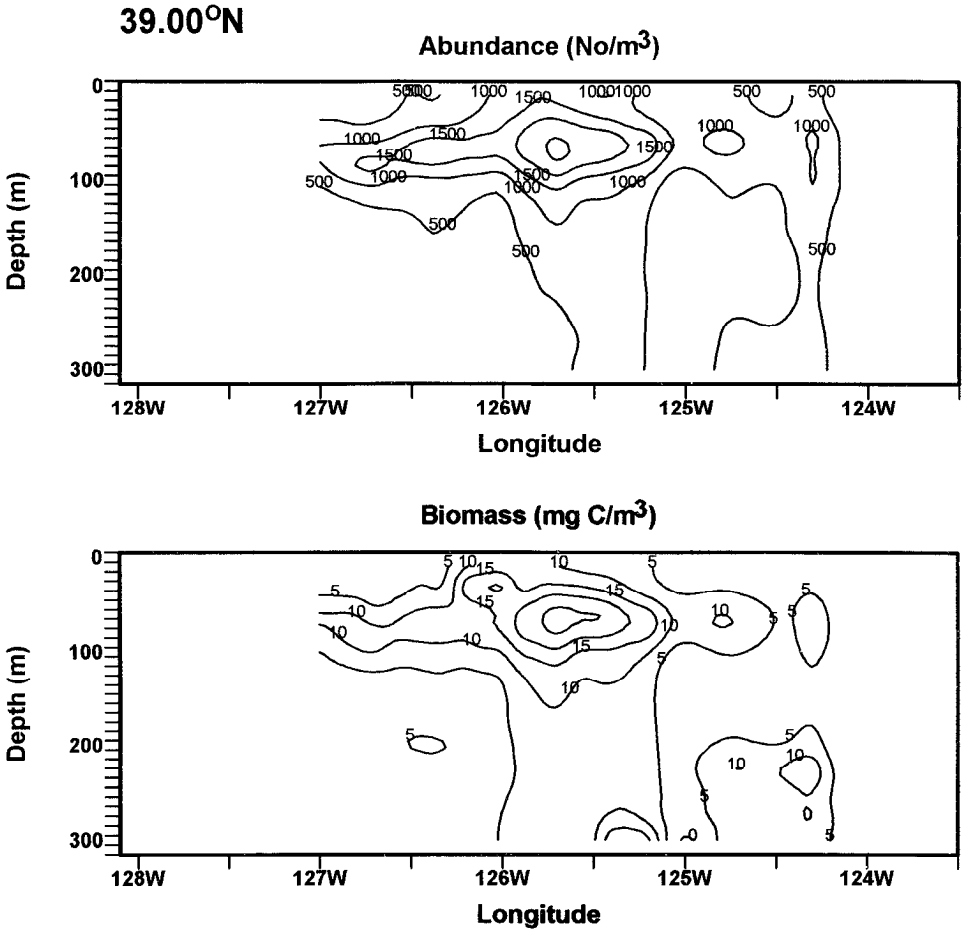

Figure 11. As in Figure 9, along 39N.

because the two survey transects south of this one (i.e. 39 and 39.25N) did not extend westward beyond 126.9W, making the dynamic topography in this area quite difficult to interpret (Fig. 1).

b. Northern coastal maximum (39.2N, 124.4W). This feature appeared to be dominated by small copepods (Fig. 8A), concentrated in a maximum that coincided with the coastal jet (Fig. 1), with abundances and biomass greatest below 100 m at 39.25N (Fig. 10). These characteristics suggest that the community here may have consisted of typically coastal species (e.g. *Paracalanus, Pseudocalanus,* and even *Calanus*), which could have been advected from the coastal upwelling regime.

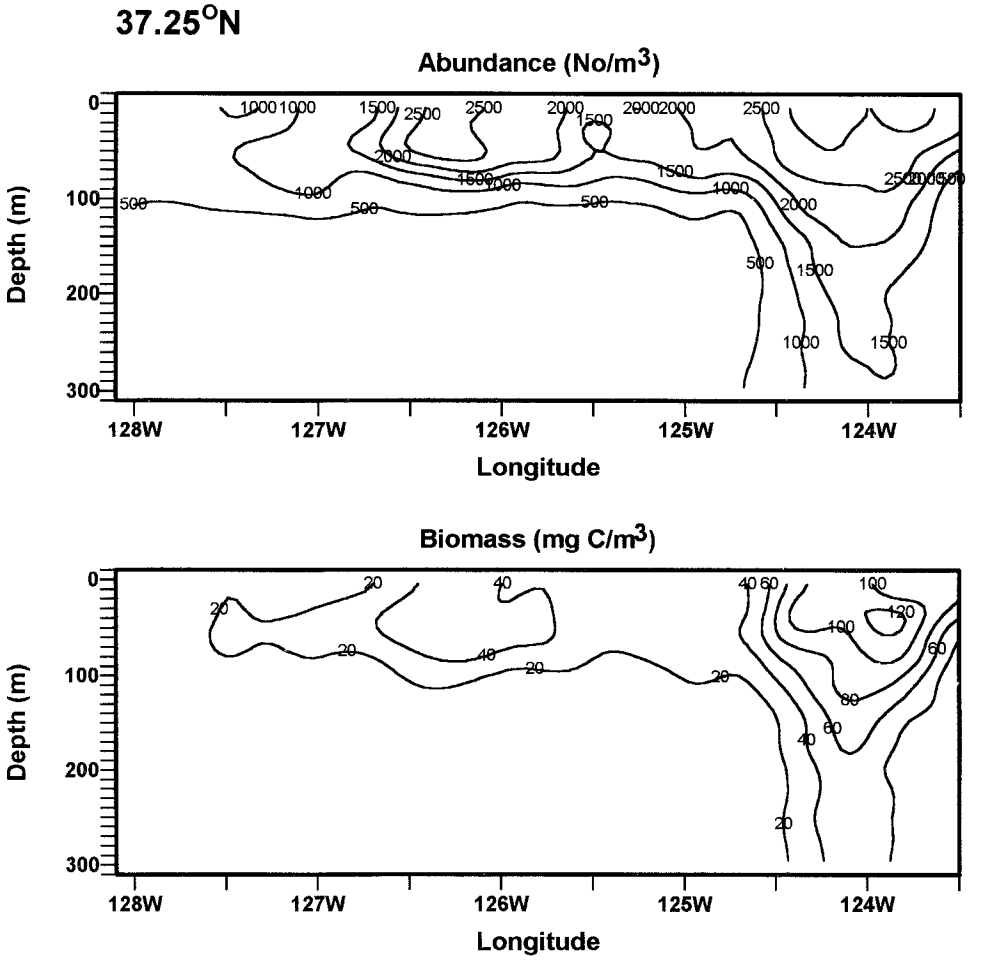

Figure 12. As in Figure 9, along 38.25N.

c. Northern anticyclonic eddy (39.2N, 125.5W). The biomass of this eddy was dominated by both small copepods (> 2.4 g C m^{-2}; Fig. 8A) and large copepods (> 1.6 g C m^{-2}; Fig. 8B), with the maxima in both abundance and biomass centered below 50 m and concentrated over a distance of 1° in longitude, or approximately 60 km (Fig. 11). Large zooplankton appeared not to constitute a significant part of the community at this location (Fig. 8C).

d. Cyclonic eddy (38.3N, 125.2W). Situated on the coastal side of the jet, the cyclonic eddy contained a high biomass of small copepods (> 1.6 g C m^{-2}; Fig. 8A), and an even greater biomass of large copepods (> 2.4 g C m^{-2}; Fig. 8B). The biomass maximum was centered above 50 m (Fig. 12), slightly more shallow than the maximum in the northern anticyclonic eddy. The results of a detailed small-scale

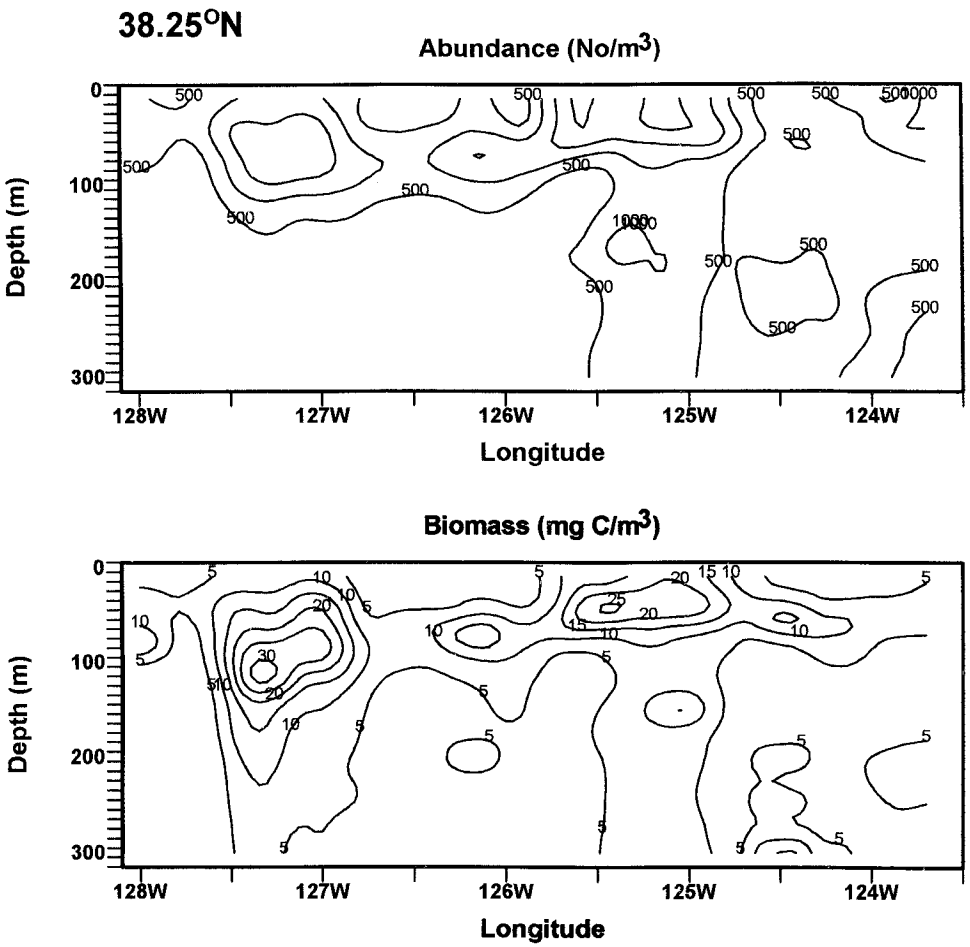

Figure 13. As in Figure 9, along 37.25N.

study, conducted in this feature and surrounding waters after the large-scale survey, are reported in a separate article (Huntley *et al.,* in preparation).

e. Central offshore maximum (38.3N, 127.4W). This feature was one of the few that was not evident in the 10-m dynamic topography with respect to 295 m (Fig. 1). Small and large copepod size categories were approximately equal in biomass (>1.6 g C m^{-2}; Figs. 8A,B). The abundance maximum was just above 100 m, while the biomass maximum was centered below it (Fig. 12), suggesting that smaller zooplankton were concentrated at shallower depths. As in the case of most mesoscale biological features observed in our study, this one was less than 1° of longitude in horizontal extent, with biomass >10 mg C m^{-3} restricted to within a diameter of ≈ 50 km (Fig. 12).

f. Coastal anticyclonic eddy (37.2N, 124W). This large feature, with total biomass of 6–20 g C m^{-2} ranging over a distance of approximately 60 km (Fig. 7), contained a large biomass of all zooplankton sizes. Small copepods were present at concentrations approaching 5 g C m^{-2}, large copepods had a biomass in the range 1.2–8.5 g C m^{-2}, and large zooplankton biomass ranged from 1.6–5 g C m^{-2} (Fig. 8A–C). Both abundance and biomass were deeply distributed; abundances $>1{,}500$ m^{-3} reached to almost 300 m, and biomass >60 mg C m^{-3} extended to almost 200 m (Fig. 13). Consistent with the observation of the importance of large zooplankton in this feature, Bongo catches yielded abundances of euphausiids that were almost as great as those observed in the northern offshore maximum at 39.5N. *Euphausia pacifica* adults dominated the species composition here, constituting 80–95% of total euphausiid abundance.

g. Southern offshore maximum (37.1N, 126.4W). A broad enhancement of zooplankton biomass in this area, 30–40 nm in extent, was dominated by both small copepods (Fig. 8A) and large zooplankton (Fig. 8C), both attaining biomass concentrations >1.6 g C m^{-2}. The biomass enhancement lay between what appears, from the dynamic topography, two weak anticyclonic eddies (Fig. 1). Unlike the coastal eddy at this same latitude, however, both the abundance and biomass of the zooplankton were concentrated in the upper 100 m (Fig. 13). The 25-km wide jet, which separated the coastal eddies from those offshore and was centered at about 124.5W at this latitude (Fig. 1), was characterized on the western side by reduced abundance and biomass of zooplankton, which increased markedly in the onshore direction (Fig. 13).

5. Discussion

We set out in this article to evaluate the application of the OPC in mapping the mesoscale distribution and abundance of zooplankton in the California Current. We first asked whether the OPC provided a reasonable estimate of abundance and biomass by comparison to a traditional capture technique using Bongo nets. We then used OPC data from a 100,000 km^2 survey conducted in June 1993 to map the vertical and horizontal distribution and abundance of zooplankton in three representative size classes, and considered the results with reference to the dynamic topography based on physical oceanographic measurements made at the same scales in time and space. We now consider the significance of these results with respect to historical observations of zooplankton in the California Current.

a. Comparison of OPC and Bongo data. We conclude that the OPC provides a valid estimate of the abundance and size-distribution of zooplankton in the region we studied. The size spectrum (normalized biomass vs. body weight) from OPC measurements over the range of body sizes equivalent to 3–3000 μg C corresponded closely to the same spectrum derived from measurements made on Bongo net samples in six

representative regions throughout the study area (Fig. 3). Furthermore, the absolute abundances estimated from both OPC and Bongo nets were also in good agreement, particularly for estimates of abundance >0.1 numbers m^{-3} (Fig. 4). In order to produce the same degree of variance as a function of the estimate of abundance, we were forced to normalize both data sets by equalizing the volume of water "filtered." As a result, it is apparent that the high variance at estimates of abundance <0.1 numbers m^{-3} was due to undersampling by both instruments. The process of normalizing filtered volumes required that our comparison of sampling methods be made at two different length scales, ≈ 2 km for the Bongo tows and 20–35 km for the OPC samples. However, autocorrelation analysis of OPC data suggested that, even at the maximum length scale of 35 km we should expect a correlation coefficient >0.5 (Fig. 2). Our approach was similar to that employed by Herman (1992) to compare net catches and OPC counts in waters on the Scotian Shelf. Despite the slight incompatibilities in horizontal scales of the two data sets, the results are highly encouraging and in our opinion strongly justify the use of the OPC for quasi-synoptic mapping of zooplankton distributions.

The taxonomic information lost by the use of the OPC is significantly compensated by the gain in horizontal and vertical resolution of measurements. Even in our standardized data set, in which seven complete vertical profiles were averaged, we obtained a composite profile every 7 km along the transect (i.e. every 35 min), with vertical resolution of 10 m. To obtain comparable resolution with a traditional net sampler would require, for example, tows of a 30-net MOCNESS (opening and closing one net in each 10-m interval) conducted more or less continuously at 35-min intervals. While such a scheme might almost be feasible, the 15,000 preserved samples it would have produced would require more than seven man-years to analyze in terms of size-composition alone, with detailed taxonomic analysis requiring additional time. We conclude that the loss in taxonomic information is more than justified by what is gained in spatial resolution by use of the OPC.

b. Temporal and spatial distribution of zooplankton in the California Current. Spatial distributions were not analyzed until we had first considered whether OPC estimates of total zooplankton standing stock in the upper 300 m could have been biased by the possibility of diel vertical migration from below. If significant numbers (or biomass) of zooplankton did perform such migrations, we would expect the average values at night to have significantly exceeded those in the day. Our analysis of the frequency distributions of both biomass and abundance in 281 day samples and 227 night samples showed no apparent difference (Fig. 5). This analysis does not, of course, preclude the possibility that vertical migration could have occurred *within* the 0–300 m stratum. However, the results allow us to conclude that vertical migration had no effect on estimates of total standing stock of zooplankton in the 0–300 m water column.

The spatial distribution of zooplankton was remarkable in several aspects. First, recognizable mesoscale features in the zooplankton distributions were strongly correlated with mesoscale features of the physical circulation. Second, the composition of these features differed with regard to absolute concentration of total biomass, and also with regard to the size categories (and therefore probably the taxonomic composition) that dominated the biomass. Third, the horizontal scale of such features was generally of order 30–60 km, which suggests that they would not be resolved by the sampling resolution employed in historical CalCOFI surveys, which is ≈ 60 nm, or one order of magnitude more coarsely resolved than the observations presented here.

The total, vertically integrated biomass of zooplankton ranged over more than one order of magnitude throughout the survey region, from < 2 g C m^{-2} to > 20 g C m^{-2} (Fig. 7). Peak concentrations were associated with both cyclonic and anticyclonic eddies. Most of these were dominated by the two smallest size fractions, with individual body weights in the range of 3–300 μg C, which we assume—based on analysis of Bongo samples—to correspond primarily to copepods. However, the greatest concentrations of biomass occurred in two locations where the largest size category (300–3000 μg C body weight), probably comprised mostly of euphausiids of 12 different species, was most abundant. One of these locations was associated with a large, coastal anticyclonic eddy west of Monterey Bay dominated by adults of *Euphausia pacifica.* At the second location, almost 200 nm offshore of Cape Mendocino at 39.5N (Figs. 7, 8C), *E. pacifica* ranked third in total abundance of 12 co-occurring species, but consisted only of late furcilia (i.e. pre-juvenile) stages.

In most of the eddies the greatest abundance and biomass of zooplankton occurred in the upper 100 m (Figs. 9–13). However, there were two notable exceptions. In the coastal anticyclonic eddy centered at 37.2N the biomass was maximal in the upper 100 m (> 120 mg C m^{-3}), but remained very high (> 60 mg C m^{-3}) to a depth of almost 200 m. The second feature of note was the coastal zooplankton maximum at 39.5N, which coincided with the location at which the central jet of the California Current departed from nearshore waters. This feature was dominated by the smallest size fraction (3–30 μg C body weight), corresponding to the size range of small copepods, and was most concentrated at depths between 100 and 300 m. In more southerly transects of the jet this feature was no longer evident.

c. Implications regarding trophic transfer. It is fair to assume that the size spectrum sampled by OPC was comprised primarily of copepods and euphausiids, which is confirmed by our examination of the Bongo samples we collected throughout the region. Until the data on distribution of phytoplankton become available (T. Cowles, Oregon State University), we make the assumption that, in general, the waters lying between the coast and the California jet contain enough particulate food to satisfy maximal growth rates of zooplankton. The studies by Checkley (1980) and Huntley

and Boyd (1984) suggest that this is a reasonable assumption. Under such circumstances, one could expect that zooplankton would grow at a rate that is limited only by temperature (Huntley and Lopez, 1992). These assumptions put us in a position to make an approximate estimate of secondary production in coastal waters of the California Current. Given that zooplankton were primarily concentrated in the upper 100 m (Figs. 9–13) where temperature was in the range of 8–16°C (A. Huyer, Oregon State University, pers. comm.), the predicted doubling rate (g) of copepods would be in the range of 0.11–0.26 d^{-1} (Huntley and Lopez, 1992). Assuming a mean temperature of 12°C (i.e. $g = 0.17\ d^{-1}$), and given a range of zooplankton biomass from 2–20 g C m^{-2}, one would predict the corresponding secondary production to be in the range of 0.34 to 3.4 g C $m^{-2}\ d^{-1}$. At the low end, this estimate represents less than one-sixth of the mean estimated primary production at more southerly locations in the California Current (Eppley *et al.,* 1985), which would quite reasonably sustain zooplankton populations with a typical gross growth efficiency of approximately 0.34 (Conover, 1978). Primary production is generally at an annual maximum during May and June off California, when it can be as high as 5 g C $m^{-2}\ d^{-1}$ (Eppley *et al.,* 1985). Admittedly, this would not likely sustain growth rates of the peak zooplankton biomass for very long, but our data show that such concentrations of zooplankton biomass were restricted to a very small area ($\approx 100\ km^2$).

d. Implications regarding spatial scales of zooplankton distribution. The overriding political reason for the advent of the California Cooperative Oceanic Fisheries Investigations (CalCOFI) was to understand the reasons for the demise of the sardine fishery. After the sardine fishery had failed, one compelling reason for the continuation of the CalCOFI program was to understand and regulate the stocks of anchovy, which was a significant fishery until the mid-1970s (California Fish and Game, 1993). Jack mackerel and Pacific mackerel fisheries assumed increasing importance during the 1980s, and Pacific sardine populations are now again on the rise. The commercial importance of these fisheries has justified continued studies of their zooplankton prey for decades. These zooplanktivorous fishes are contagiously distributed at scales that reflect their exploitation of prey resources (MacCall, 1990), so it would seem to make sense that the distributions of their prey—at least—should be studied at spatial scales where the greatest variability is expected. The results of this study in the central California Current show, for the first time, that the characteristic synoptic scale of variability in zooplankton distributions is of order 30–60 km. This is the spatial scale that corresponds to changes in physical forcing (i.e. eddies, upwelling) on time scales of weeks to months (Haury *et al.,* 1978), which in turn correspond to the time scale of zooplankton populations at these latitudes, as defined by their generation time (Huntley and Lopez, 1992). Thus, it is the mesoscale pattern of distribution of zooplankton that most accurately reflects their population dynamics and thus their susceptibility to predation. Until this scale is adequately

sampled, many of the underlying causes for variability in the commercial fisheries of California will probably continue to elude us.

Acknowledgments. This research was supported by Office of Naval Research grant number NOO014-92-J-1618. We are grateful to F. Carlotti, A. Gonzalez and M. D. G. Lopez for their invaluable assistance in shipboard research activities, and to the two former individuals for their efforts in processing some of the preserved samples of zooplankton. We thank Y. Zhu for her monumental effort in preparing and analyzing the standardized OPC database, E. Brinton for his help in identifying key euphausiid species, J. Barth, A. Huyer, M. Kosro and R. L. Smith for use of their physical oceanographic data, N. Potter for his limitless creative suggestions, and the crew and technical support personnel (particularly M. Willis, M. Hill and T. Holt) of the R/V *Wecoma* for their expert help with the SeaSoar. This is contribution no. 7 of the Simon J. Poole Institute.

REFERENCES

Banse, K. 1964. On the vertical distribution of zooplankton in the sea. Prog. Oceanogr., *2,* 55–125.

Barnett, A. M. 1974. The feeding ecology of an omnivorous neritic copepod, *Labidocera trispinosa* Esterly. Ph.D. dissertation, University of California San Diego, 215 pp.

Bernstein, R. L., L. Breaker and R. Whritner. 1977. California Current eddy formation: Ship, air and satellite results. Science, *195,* 353–359.

Bretherton, F. P., R. E. Davis and C. B. Fandry. 1976. A technique for objective analysis and design of oceanographic experiments applied to MODE-73. Deep-Sea Res., *23,* 559–582.

Brinton, E. 1962. The distribution of Pacific euphausiids. Bull. Scripps Inst. Oceanogr., *8,* 51–270.

California Department of Fish and Game 1993. Review of some California fisheries for 1992. CalCOFI Reports, *34,* 7–20.

Carter, E. F. and A. Robinson. 1987. Analysis models for the estimation of oceanic fields. J. Atmos. Ocean Tech., *4,* 49–75.

Checkley, D. M., Jr. 1980. The egg production of a marine planktonic copepod in relation to its food supply: laboratory studies. Limnol. Oceanogr., *25,* 430–446.

Clancy, R. M. 1983. The effect of observational error correlations on objective analysis of ocean thermal structure. Deep-Sea Res., *30,* 985–1002.

Conover, R. J. 1978. Transformation of organic matter, *in* Marine Ecology, O. Kinne, ed., Dynamics 4. Wiley-Interscience, Chichester, 221–499.

Eppley, R. W., E. Stewart, M. R. Abbott and U. Heyman. 1985. Estimating ocean primary production from satellite chlorophyll. Introduction to regional differences and statistics for the Southern California Bight. J. Plankton Res., *7,* 57–70.

Fleminger, A. 1964. Distribution atlas of calanoid copepods in the California Current region, Part I. California Cooperative Oceanic Fisheries Investigations, State of California, 313 pp.

Frost, B. W. 1980. The inadequacy of body size as an indicator of niches in the zooplankton, *in* Evolution and Ecology of Zooplankton Communities, W. C. Kerfoot, ed., University Press of New England, Hanover, N.H., 742–753.

Fulton, J. 1973. Some aspects of the life history of *Calanus plumchrus* in the Strait of Georgia. J. Fish. Res. Bd. Canada, *30,* 811–815.

Haury, L. 1984. An offshore eddy in the California Current system, part IV: Plankton distributions. Prog. Oceanogr., *13,* 95–111.

Haury, L. R., J. A. McGowan and P. H. Wiebe. 1978. Patterns and processes in time-space scales of plankton distributions, *in* Spatial Patterns in Plankton Communities, J. H. Steele, ed., Plenum Press, London, 277–328.

Herman, A. W. 1988. Simultaneous measurement of zooplankton and light attenuance with a new optical plankton counter. Cont. Shelf Res., *8,* 205–221.

—— 1992. Design and calibration of a new optical plankton counter capable of sizing small zooplankton. Deep-Sea Res., *39,* 395–415.

Hickey, B. 1979. The California Current system—hypotheses and facts. Prog. Oceanogr., *8,* 191–279.

Huntley, M. and C. Boyd. 1984. Food-limited growth of marine zooplankton. Am. Nat., *124,* 455–478.

Huntley, M. E. and M. D. G. Lopez. 1992. Temperature-dependent production of marine copepods: a global synthesis. Am. Nat., *140,* 201–242.

Huyer, A., P. M. Kosro, J. Fleischbein, S. R. Ramp, T. Stanton, L. Washburn, F. P. Chavez, T. J. Cowles, S. D. Pierce and R. L. Smith. 1991. Currents and water masses of the coastal transition zone off northern California, June to August, 1988. J. Geophys. Res., *96,* 14809–14831.

Kosro, P. M., A. Huyer, J. Barth, R. L. Smith and P. T. Strub. 1994. Eddies in the California Current region off northern California from satellite and SeaSoar/ADCP measurements. EOS, *75,* 140.

Kosro, P. M., A. Huyer, S. R. Ramp, R. L. Smith, F. P. Chavez, T. J. Cowles, M. R. Abbott, P. T. Strub, R. T. Barber, P. Jessen and L. F. Small. 1991. The structure of the transition zone between coastal waters and the open ocean off northern California, winter and spring 1987. J. Geophys. Res., *96,* 14707–14730.

Landry, M. R. 1983. The development of marine calanoid copepods with comment on the isochronal rule. Limnol. Oceanogr., *28,* 614–624.

MacCall, A. D. 1990. Dynamic Geography of Marine Fish Populations. University of Washington Press, Seattle, 153 pp.

Mackas, D. L., L. Washburn and S. L. Smith. 1991. Zooplankton community pattern associated with a California Current cold filament. J. Geophys. Res., *96,* 14781–14797.

Miller, C. B., J. K. Johnson and D. R. Heinle. 1977. Growth rules in the marine copepod genus *Acartia.* Limnol. Oceanogr., *22,* 326–335.

Mooers, C. N. K. and A. R. Robinson. 1984. Turbulent jets and eddies in the California Current and inferred cross-shore transports. Science, *223,* 51–53.

Mullin, M. M. and E. R. Brooks. 1970. Growth and metabolism of two planktonic, marine copepods as influenced by temperature and type of food, *in* Marine Food Chains, J. H. Steele, ed., Oliver and Boyd, Edinburgh, 74–95.

Ohman, M. D. 1985. Resource-satiated population growth of the copepod *Pseudocalanus* sp. Arch. Hydrobiol. Beih. Ergebn. Limnol., *21,* 15–32.

Peláez, J. and J. A. McGowan. 1986. Phytoplankton pigment patterns in the California Current as determined by satellite. Limnol. Oceanogr., *31,* 927–950.

Platt, T. and K. Denman. 1978. The structure of pelagic marine ecosystems. Rapp. P.-v. Réun. Cons. Int. Explor Mer, *173,* 60–65.

Poulain, P. and P. P. Niiler. 1989. Statistical analysis of the surface circulation in the California Current system using satellite-tracked drifters. J. Phys. Oceanogr., *19,* 1588–1603.

Robinson, A. R., J. A. Carton, C. N. K. Mooers, L. J. Walstad, E. F. Carter, M. M. Rienecker, J. A. Smith and W. G. Leslie. 1984. A real-time dynamical forecast of ocean synoptic/mesoscale eddies. Nature, *309,* 781–783.

Rodríguez, J. and M. M. Mullin. 1986. Relation between biomass and body weight of plankton in a steady state oceanic ecosystem. Limnol. Oceanogr., *31,* 361–370.

Smith, P. E. 1974. Distribution of zooplankton volumes in the California Current region, 1969. California Cooperative Oceanic Fisheries Investigations, State of California, 118–125.

Smith, S. L. and P. V. Z. Lane. 1991. The jet off Point Arena, California: its role in aspects of secondary production in the copepod *Eucalanus californicus.* J. Geophys. Res., *96,* 14849–14858.

Sprules, W. G., S. B. Brandt, D. J. Stewart, M. Munawar, E. H. Jin and J. Love. 1991. Biomass size spectrum of the Lake Michigan pelagic food web. Can. J. Fish. Aquat. Sci., *48,* 105–115.

Sverdrup, H. U., M. W. Johnson and R. H. Fleming. 1946. The Oceans, Their Physics, Chemistry and General Biology. Prentice-Hall, New York, 1087 pp.

Vidal, J. and S. L. Smith. 1986. Biomass, growth, and development of populations of herbivorous zooplankton in the southeastern Bering Sea during spring. Deep-Sea Res., *33,* 523–556.

Wyllie, J. G. 1966. Geostrophic flow of the California Current at the surface and at 200 m. California Cooperative Oceanic Fisheries Investigations, State of California, 12 pp.

Received: *5 October, 1994;* revised: *16 February, 1995.*